

## Density Functional Theory and Molecular Docking Analysis of Newly Synthesized and Characterized Benzimidazolium Salts

Elvan Üstün<sup>1</sup> , Neslihan Şahin<sup>2</sup> 

Ordu University, Faculty of Art and Science, Department of Chemistry, Ordu  
Cumhuriyet University, Faculty of Education, Department of Mathematics and Science Education, Sivas

Geliş Tarihi / Received Date: 17.05.2022 Kabul Tarihi / Accepted Date: 18.06.2022

### Abstract

Benzimidazoles, an important member of the N-heterocyclic carbenes family, draw attention to their catalytic properties as well as their pharmaceutical activity. Since these molecules are relatively easy to synthesize and derivatize, they are frequently used in the synthesis of species with desired properties and metal complexes of these species. The interactions of these kinds of pharmaceutical molecules with the tissue and blood components are important. The interaction of the bioactive species with serum albumin, which is one of the most important proteins in the blood, is a frequently studied subject and Bovine Serum Albumin is frequently used in these researches. In-silico methods provide many advantages and give important insights before experimental procedures. In this study, two novel benzimidazolium salts were synthesized and characterized. After the structural analysis of the molecules was analyzed by DFT-based calculation methods, the reactivities of the molecules were also examined with Global Reactivity Descriptors. In addition, the interactions of molecules with Bovine Serum Albumin were analyzed by molecular docking methods.

**Keywords:** N-heterocyclic carbenes, molecular docking, DFT, benzimidazole, bovine serum albumin

## Yeni Sentezlenmiş ve Karakterize Edilmiş Benzimidazolyum Tuzlarının Yoğunluk Fonksiyonel Teorisi ve Moleküler Doking Analizi

### Öz

N-heterosiklik karbenler ailesinin önemli bir üyesi olan benzimidazoller, farmasötik aktivitelerinin yanı sıra katalitik özellikleri ile de dikkat çekmektedir. Bu moleküllerin sentezlenmesi ve türevlendirilmesi nispeten kolay olduğundan, bu bileşikler istenen özelliklere sahip yeni türlerin ve bu türlerin metal komplekslerinin sentezinde sıklıkla kullanılırlar. Bu tür farmasötik moleküllerin doku ve kan bileşenleri ile etkileşimleri önemlidir. Biyoaktif türlerin kandaki en önemli proteinlerden biri olan serum albümini ile etkileşimi sıkça çalışılan bir konudur ve bu araştırmalarda Sığır Serum Albümin sıklıkla kullanılmaktadır. In-siliko yöntemler birçok avantaj sağlar ve deneysel prosedürlerden önce önemli bilgiler verir. Bu çalışmada iki yeni benzimidazolyum tuzu sentezlenmiş ve karakterize edilmiştir. Moleküllerin yapısal analizi DFT tabanlı hesaplama yöntemleri ile analiz edildikten sonra, Global Reaktivite Tanımlayıcıları ile moleküllerin reaktiviteleri de incelenmiştir. Ayrıca moleküllerin Sığır Serum Albümin ile etkileşimleri moleküler doking yöntemleri ile analiz edildi.

**Anahtar Kelimeler:** N-heterosiklik karbenler, moleküler doking, DFT, benzimidazol, sığır serum albümini

## Introduction

N-heterocyclic carbenes have found a number of applications in important processes due to their catalytic activities since firstly isolated and characterized in 1991 (Arduengo et al., 1991; Nair et al., 2008). One of the important members of this family is benzimidazoles which have been frequently studied by the scientific world for many years due to their stability, reactivity, basicity, and high polar properties (Barot et al., 2013; Spasov et al., 1999; Yadav & Ganguly, 2015). The catalytic activity of these molecules is well known and benzimidazole derivative dyes are also reported (Manoharan & Anandan, 2014). Benzimidazoles can bind to proteins, enzymes, and receptors in biological systems by H-bonds and proton donor/acceptor properties since they contain two nitrogen atoms and are frequently used in medicinal chemistry applications (Narasimhan et al., 2012; Velik et al., 2004;).

Benzimidazole derivative molecules used as anthelmintic (albendazole, mebendazole, triclabendazole etc.), fungicide (benomyl, carbendazim, thiabendazole etc.), proton pump inhibitor (omeprazole, lansoprazole, pantoprazole, rabeprazole, and tenatoprazole etc.) (Law & Yeong, 2021).

Serum Albumin, commonly known as blood albumin, is the most abundant dissolved protein in blood plasma (Goldwasser & Feldman, 1997). Albumin is essential for delivering of necessary components by body fluids to the tissues with blood vessels. It is important to analyze the interaction of the molecules with albumin which transports hormones, hemin, and fatty acids in the plasma (Peters, 1985). Bovine Serum Albumin which is chemically similar with Human Serum Albumin is usually used in experimental studies since it is more attainable.

Recent developments in theoretical and computational chemistry give important insights about the structural properties of the molecules and their interactions with biological macromolecules (Serdaroğlu et al., 2021; Şahin et al., 2021). The theoretical results agree with the experimental results and this kind of analysis saves budget, labor, and time. In this study, two new benzimidazolium salts were synthesized and characterized by  $^1\text{H}$  NMR,  $^{13}\text{C}$  NMR, and FT-IR methods, and the characterization of molecules was completed by UV-Vis spectroscopy. After the structural analysis of the molecules was analyzed with DFT-based calculation methods, the reactivities of the molecules were examined with Global Reactivity Descriptors. In addition, the interactions of molecules with Bovine Serum Albumin were analyzed by molecular docking methods.

## Material and Method

### Experimental Synthesis

Standard Schlenk line techniques were used for all synthesis procedures under argon atmosphere with flame-dried glassware. All reagents are Sigma Aldrich (Dorset, UK). Purification of all solvents was done by distillation methods over the drying agents, and they were transferred to the reaction matrix under Argon. Electrothermal 9100 was used for melting point detection by capillary tubes. Perkin Elmer Spectrum 100 FT-IR was used for recording the Fourier transform infrared (FT-IR) spectra in the range 400–4000  $\text{cm}^{-1}$ .  $^1\text{H}$  NMR and  $^{13}\text{C}\{^1\text{H}\}$  NMR spectra were taken using a Bruker As 400 Mercury spectrometer operating at 400 MHz ( $^1\text{H}$ ), 100 MHz ( $^{13}\text{C}$ ) in  $\text{CDCl}_3$  with tetramethylsilane as the internal reference. UV-Vis spectra were also recorded by Shimadzu UV-1800 Spectrophotometer.

### **Preparation of 1-allyl-3-(4-tert-butylbenzyl)-5,6-dimethylbenzimidazolium bromide, 1**

According to the previous study, compound **1** was synthesized under argon gas atmosphere (Şahin et al., 2021). To a stirring solution of NaH (11 mmol) in tetrahydrofuran (20 mL), 5,6-dimethylbenzimidazole (10 mmol) was added and the admixture was stirred at room temperature for 1 h. Then, allyl bromide (10.1 mmol) was added to the solution and the mixture was left to stir for 24 h at 60 °C. The mixture was cooled to room temperature. Then, the solvent was removed in vacuo. Dichloromethane (30 mL) was added to the solid. The last solution was distilled and 1-allyl-5,6-dimethylbenzimidazole was obtained. The 1-allyl-5,6-dimethylbenzimidazole (1 mmol) and 4-tert-butylbenzyl bromide (1 mmol) were stirred in DMF (5 mL) for 24 h at 80 °C. Precipitated solid was

filtered and rinsed out with diethyl ether and dried under the vacuum. Yield: 84%; m.p. 178-179 °C, FT-IR  $\nu_{(\text{CN})}$ : 1561  $\text{cm}^{-1}$ .  $^1\text{H}$  NMR (400 MHz,  $\text{CDCl}_3$ )  $\delta$  (ppm): 1.27 (s, 9H,  $\text{CH}_2\text{C}_6\text{H}_4\text{-C}(\text{CH}_3)_3\text{-4}$ ), 2.40, 2.41 (s, 6H,  $\text{NC}_6\text{H}_2\text{N}(\text{CH}_3)_2\text{-5,6}$ ), 5.26 (d, 2H,  $\text{NCH}_2\text{CHCH}_2$ ,  $J=8$  Hz), 5.44 (s, 1H,  $\text{NCH}_2\text{CHCH}_2$ ), 5.47 (d, 1H,  $\text{NCH}_2\text{CHCH}_2$ ,  $J=8$  Hz), 5.76 (s, 2H,  $\text{CH}_2\text{C}_6\text{H}_4\text{-C}(\text{CH}_3)_3\text{-4}$ ), 6.11 (quint, 1H,  $\text{NCH}_2\text{CHCH}_2$ ,  $J=4$  Hz), 7.37-7.40 (m, 3H, Ar-H), 7.43-7.46 (m, 3H, Ar-H), 11.38 (s, 1H, NCHN).  $^{13}\text{C}\{^1\text{H}\}$  NMR (100 MHz,  $\text{CDCl}_3$ )  $\delta$  (ppm): 20.7 ( $\text{NC}_6\text{H}_2\text{N}(\text{CH}_3)_2\text{-5,6}$ ), 31.2 ( $\text{CH}_2\text{C}_6\text{H}_4\text{-C}(\text{CH}_3)_3\text{-4}$ ), 34.7 ( $\text{CH}_2\text{C}_6\text{H}_4\text{-C}(\text{CH}_3)_3\text{-4}$ ), 50.0 ( $\text{NCH}_2\text{CHCH}_2$ ), 50.9 ( $\text{CH}_2\text{C}_6\text{H}_4\text{-C}(\text{CH}_3)_3\text{-4}$ ), 126.3 ( $\text{NCH}_2\text{CHCH}_2$ ), 137.4 ( $\text{NCH}_2\text{CHCH}_2$ ), 113.2, 113.4, 121.6, 128.1, 129.7, 129.9, 130.0, 152.3 (Ar-C), 141.6 (NCHN).

### Preparation of 1-allyl-3-(4-methoxybenzyl)-5,6-dimethylbenzimidazolium chloride, 2

**2** was prepared following the same procedures as described for **1**. However, 4-methoxybenzyl chloride (1 mmol) was used as second added alkyl halide. Yield: 81%; m.p. 209-210 °C, FT-IR  $\nu_{(\text{CN})}$ : 1557  $\text{cm}^{-1}$ .  $^1\text{H}$  NMR (400 MHz,  $\text{CDCl}_3$ )  $\delta$  (ppm): 2.40 (s, 6H,  $\text{NC}_6\text{H}_2\text{N}(\text{CH}_3)_2\text{-5,6}$ ), 3.75 (s, 3H,  $\text{CH}_2\text{C}_6\text{H}_4\text{-OCH}_3\text{-4}$ ), 5.27 (s, 2H,  $\text{NCH}_2\text{CHCH}_2$ ), 5.43 (d, 2H,  $\text{NCH}_2\text{CHCH}_2$ ,  $J=16$  Hz), 5.76 (s, 2H,  $\text{CH}_2\text{C}_6\text{H}_4\text{-OCH}_3\text{-4}$ ), 6.09 (quint, 1H,  $\text{NCH}_2\text{CHCH}_2$ ,  $J=4$  Hz), 6.85-6.87 (m, 2H, Ar-H), 7.42-7.44 (m, 2H, Ar-H), 7.48-7.50 (m, 2H, Ar-H), 11.31 (s, 1H, NCHN).  $^{13}\text{C}\{^1\text{H}\}$  NMR (100 MHz,  $\text{CDCl}_3$ )  $\delta$  (ppm): 20.7 ( $\text{NC}_6\text{H}_2\text{N}(\text{CH}_3)_2\text{-5,6}$ ), 49.9 ( $\text{NCH}_2\text{CHCH}_2$ ), 50.8 ( $\text{CH}_2\text{C}_6\text{H}_4\text{-OCH}_3\text{-4}$ ), 55.3 ( $\text{CH}_2\text{C}_6\text{H}_4\text{-OCH}_3\text{-4}$ ), 125.2 ( $\text{NCH}_2\text{CHCH}_2$ ), 137.3 ( $\text{NCH}_2\text{CHCH}_2$ ), 113.2, 113.4, 114.6, 121.2, 125.2, 129.9, 128.1, 130.0, 160.0 (Ar-C), 141.9 (NCHN).

### Calculation Method

Full unconstrained geometry optimizations with DFT-based calculation methods were carried out with ORCA version 4.2 using the exchange functional according to BP86 that the correlation functional suggested by Becke and Perdew, with the resolution-of-the-identity (RI) approximation, the tightscf, KDIIS, and SOSCF options, a def2-SVP basis set (Becke, 1988; Furche & Perdew, 2006; Neese, 2012; Neese, 2018; Serdaroğlu et al., 2022). To speed up the calculations def2-SVP/J auxiliary basis set was used.

All the global chemical reactivity descriptors were calculated with Koopmans Theorem according to the following equations (Phillips, 1961):

$$IP = -E_{HOMO} \quad (1)$$

$$EA = -E_{LUMO} \quad (2)$$

$$\chi = -\frac{IP + EA}{2} \quad (3)$$

$$\eta = \frac{IP - EA}{2} \quad (4)$$

$$S = \frac{1}{2\eta} \quad (5)$$

$$\omega = \frac{\mu^2}{2\eta} \quad (6)$$

Where IP is ionization potential; EA is electron affinity;  $\chi$  is electronegativity;  $\eta$  is global hardness; S is global softness; and  $\omega$  is electrophilicity index (Vijayaraj et al., 2009).

AutoDockTools 4.2 were used for molecular docking calculations with crystal structure from the RCSB protein data bank (PDB ID: 4f5s, <https://www.rcsb.org/structure/4F5S>) (Bujacz, 2012). Only polar hydrogens and Kollman charges were evaluated in target molecules and the waters in proteins were removed. Randomized starting positions, Gasteiger charges, and torsions have been evaluated for ligand molecules. While Lamarckian genetic algorithms were applied, the genetic algorithm population was recorded as 150. Discovery Studio 4.1.0 was used for illustrations (Dassault Systèmes, 2016).

## Result and Discussion

### Synthesis and characterization of benzimidazolium salts

Benzimidazolium salts (**1** and **2**) were synthesized by reaction of 1-allyl-5,6-dimethylbenzimidazole with 4-*ter*-butylbenzyl bromide and 4-methoxybenzyl chloride in DMF at 80 °C, respectively as shown Figure 1. The precipitated products were crystallized in dichloromethane/diethyl ether for purification. The structure of the new compounds is characterized by FT-IR,  $^1\text{H}$  NMR,  $^{13}\text{C}\{^1\text{H}\}$  NMR, and UV-Vis spectroscopy.

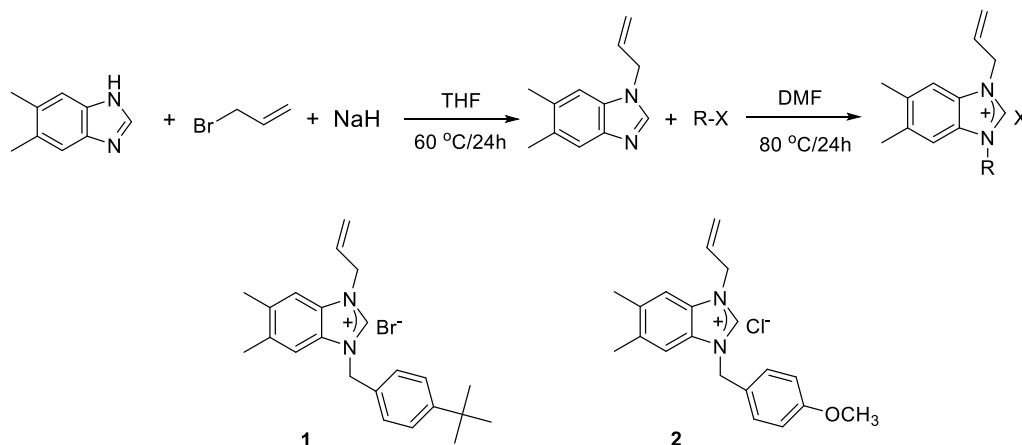


**Figure 1.** Synthesis of Benzimidazolium Salts **1** and **2**

It was observed that all C-H stretching vibrational bands peaked between 2700-3100  $\text{cm}^{-1}$  at the IR spectra of the benzimidazolium salts. C=C stretching vibrational bands were seen at around 1800-1600  $\text{cm}^{-1}$ . Specific CN peaks in the benzimidazolium ring were observed at 1561  $\text{cm}^{-1}$  and 1557  $\text{cm}^{-1}$  for **1** and **2**, respectively.

NMR spectra of the compounds were analyzed in  $d\text{-CDCl}_3$ . In the  $^1\text{H}$  NMR spectra, the NCHN acidic protons of **1** and **2** were seen at 11.38 ppm and 11.31 ppm as sharp singlets, respectively. For both compounds, the methyl protons of benzimidazole peaked in the range of 2.20 ppm and 2.40 ppm as singlets. Benzylic protons were seen at 5.76 ppm as singlets for both salts. Protons of  $\text{NCH}_2\text{CHCH}_2$  of salts (**1** and **2**) came at 6.11 ppm and 6.09 ppm as a quint, respectively. Aromatic protons of salts **1** and **2** were observed in the range of 6.85-7.50 ppm.

In the  $^{13}\text{C}\{^1\text{H}\}$  NMR spectra, NCHN carbons of benzimidazolium salts give the peak at 141.6 ppm and 141.9 ppm, respectively **1** and **2**. Aromatic carbons of compounds **1** and **2** were seen in the range of 113.0-160.0 ppm. Benzylic carbons of **1** and **2** gave peaks at 50.9 ppm and 50.8 ppm, respectively. The methyl carbon peaks of benzimidazole of the compounds were observed at around 20.0 ppm. These values are in agreement with reported data for similar compounds (Şahin et al., 2021). The FT-IR,  $^1\text{H}$  NMR,  $^{13}\text{C}\{^1\text{H}\}$  NMR, and UV-Vis spectra are presented in Figures 2-6.

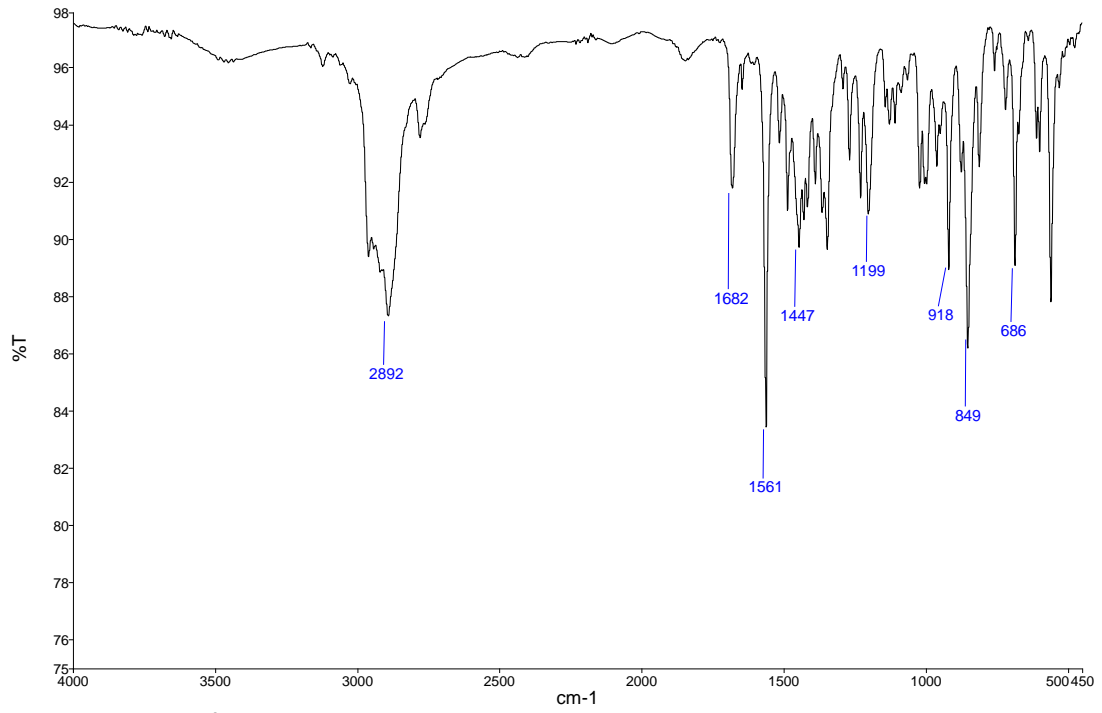


**Figure 2.** FT-IR Spectra of 1

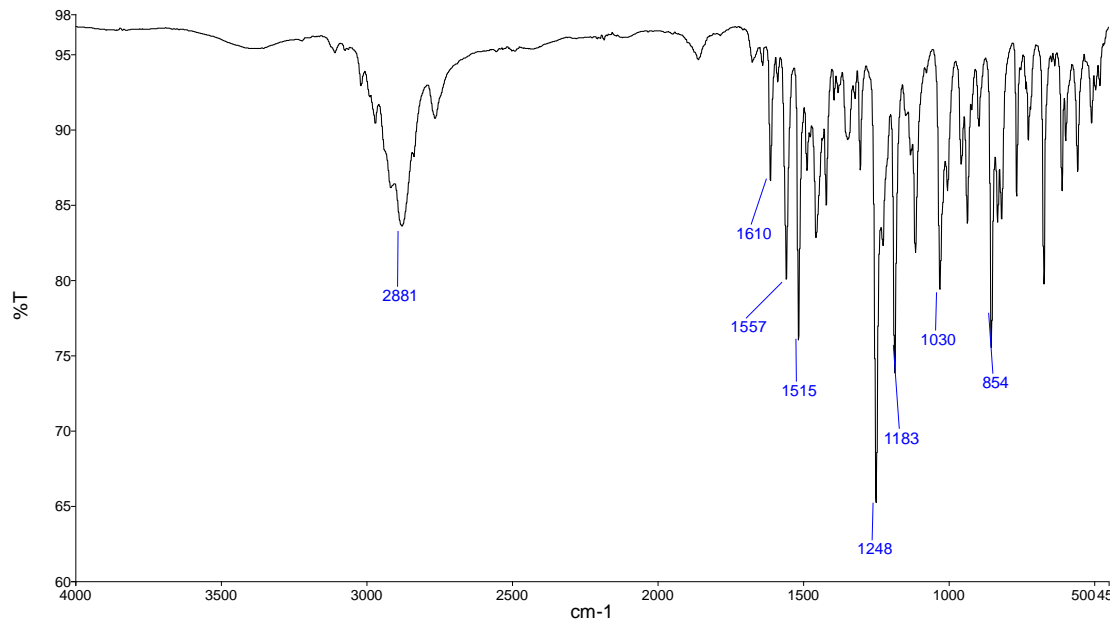


**Figure 3.** FT-IR Spectra of 2

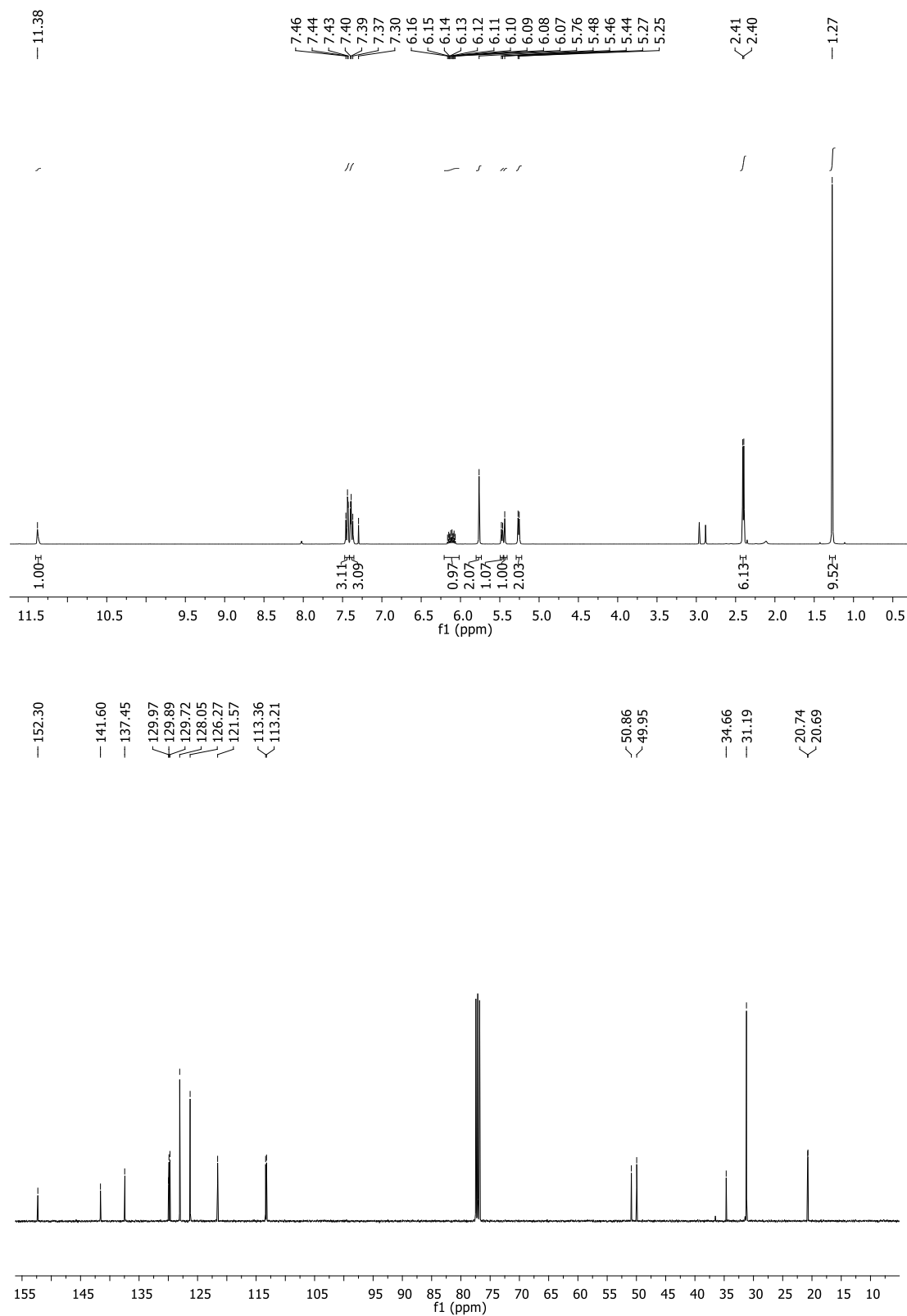


Figure 4. <sup>1</sup>H NMR and <sup>13</sup>C{<sup>1</sup>H} NMR Spectra of 1

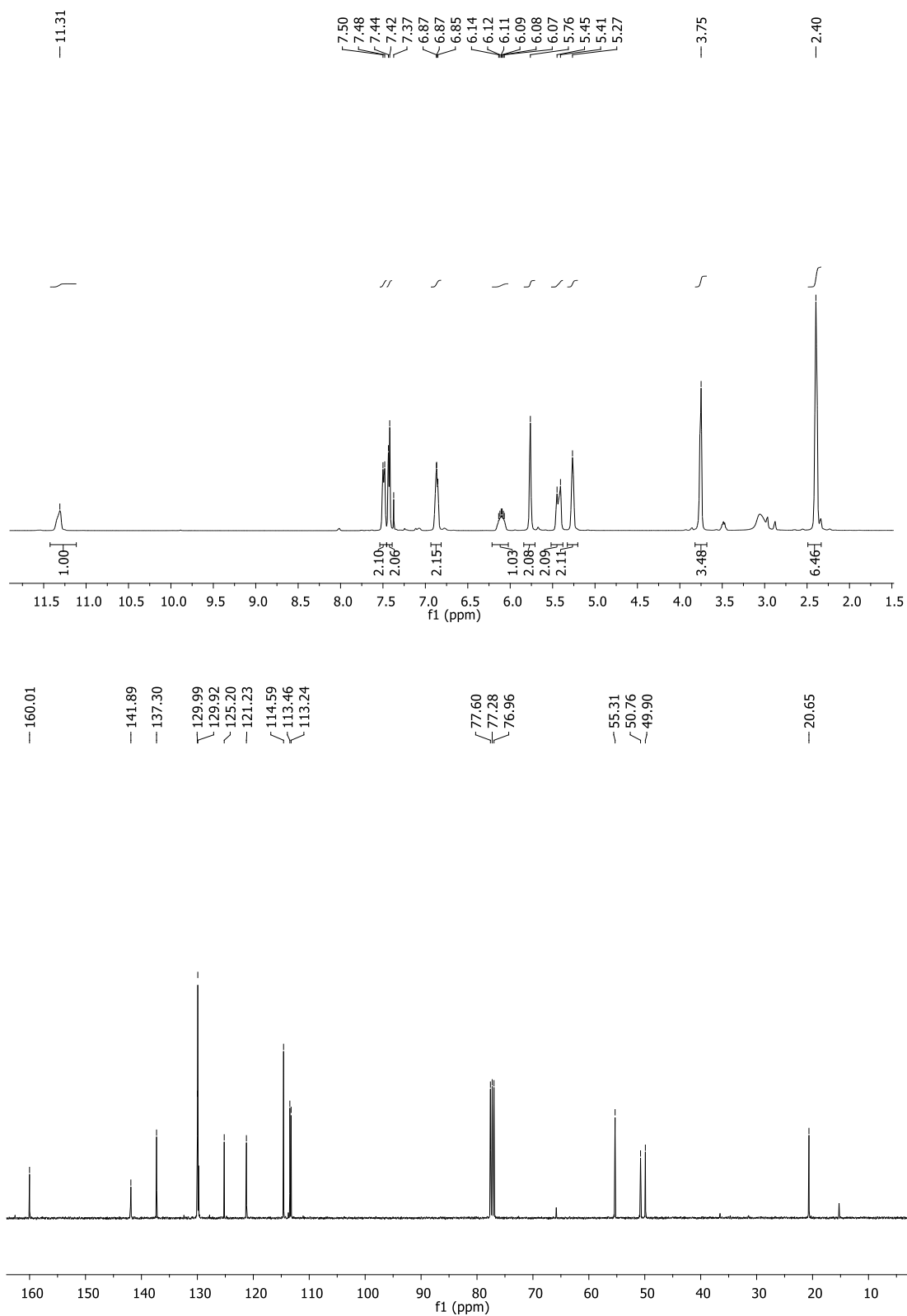
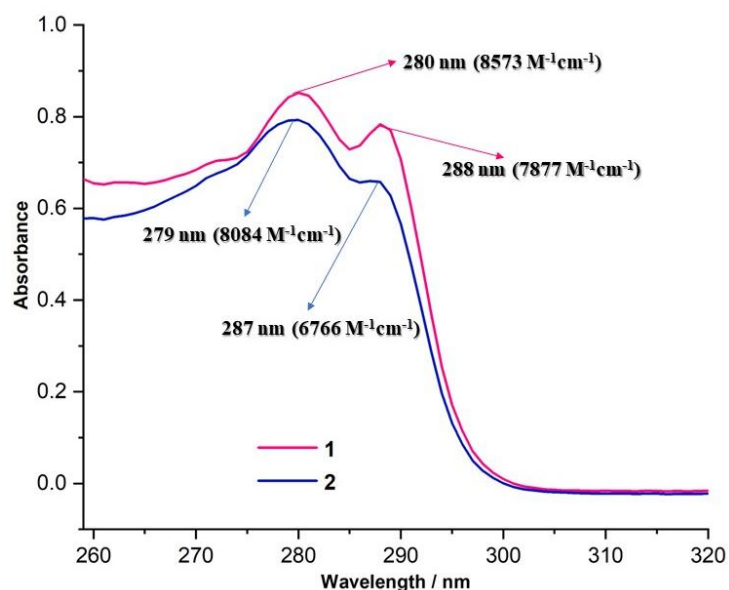
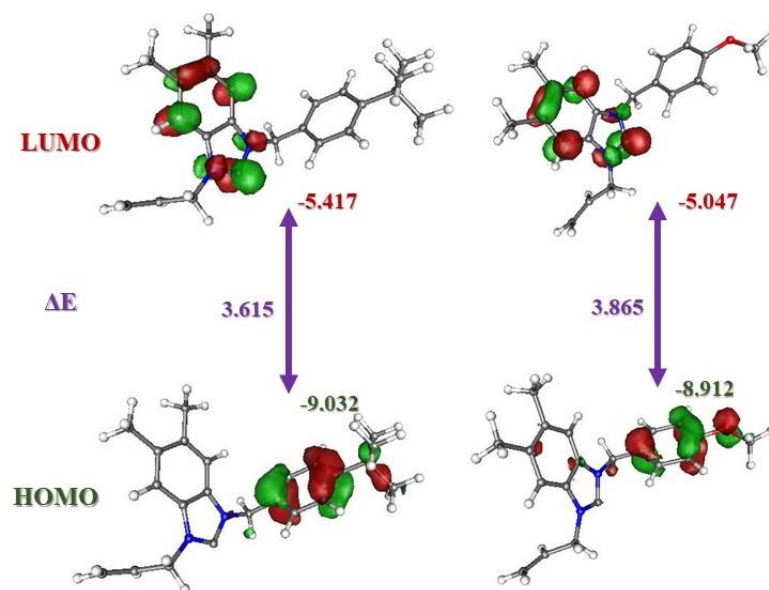


Figure 5. <sup>1</sup>H NMR and <sup>13</sup>C{<sup>1</sup>H} NMR Spectra of 2



**Figure 6.** UV-Vis Spectra of 1 and 2 (The Extinction Coefficients of the Bands Given in Parenthesis)

UV-Vis spectrophotometer is an important method in the analysis of possible-pharmaceutical molecules. The methanol solutions of the molecules were prepared, and their spectra were recorded. Solutions of the molecules are colorless and show two main bands in the UV-Vis spectra. While bands were recorded at 279 nm and 288 nm for **1**, molecule **2** shows two maxima at 279 nm and 287 nm. The extinction coefficients of these bands were determined by recording the spectra of the solutions prepared as three sets in five different concentrations (Figure 7).



**Figure 7.** HOMO and LUMO Energies and Illustrations of the Molecules (in eV)

### Theoretical analysis

The location and energy of the Highest Occupied Molecular Orbital (HOMO) and Lowest Unoccupied Molecular Orbital (LUMO) of the molecules are important in the reactivity analysis of the molecules. The HOMO region of the molecule indicates the region where electron-donating reactions will take place, while the LUMO shows the region where the molecule accepts electron (Bejaoui et al., 2020). According to this evaluation, it is expected to act as an electron donor through the benzyl region of benzimidazole in both molecules. On the other hand, in both molecules, it is expected to exhibit



electron acceptor properties through the conjugated benzimidazole group (Figure 7). The relative energies of the HOMO and LUMO of the molecules give quantitative idea about the electron donor and acceptor flairs of the molecules (Perepichka & Bryce, 2005). According to the DFT-based calculations, **1** acts as an efficient electron donor since the HOMO has lower energy. At the same time, **1** shows more effective electron acceptor property since it has lower LUMO energy.

**Table 1.** Global Reactivity Descriptors of the Complexes (in eV)

	1	2
Ionization Potential (IP)	9.032	8.912
Electron Affinity (EA)	5.417	5.047
Electronegativity ( $\chi$ )	7.224	6.979
Global Softness (S)	0.277	0.259
Global Hardness ( $\eta$ )	1.807	1.932
Electrophilicity Index( $\omega$ )	14.456	12.615

Global Reactivity Descriptors were calculated by using the energies of the HOMO and LUMO of molecules according to the Koopman Theorem which is frequently used in the analysis of the electron donor/acceptor properties of molecules (Phillips, 1961; Vijayaraj et al., 2009). According to this theorem, the calculated IP and EA values for molecules are obtained by direct evaluation of the HOMO and LUMO energies of the molecules. According to the results, **1** is expected to be more active in terms of both electron-donor and electron-acceptor properties due to higher IP and EA values and **1** also shows stronger electronegativity. The larger global softness value and the smaller global hardness value indicate the more reactive molecule. In this case, **1** is expected to be more reactive. The electrophilicity index is the expression of the affinity of a molecule against an electrophile, and the electrophilicity index of **1** was calculated greater than 2 (Table 1).

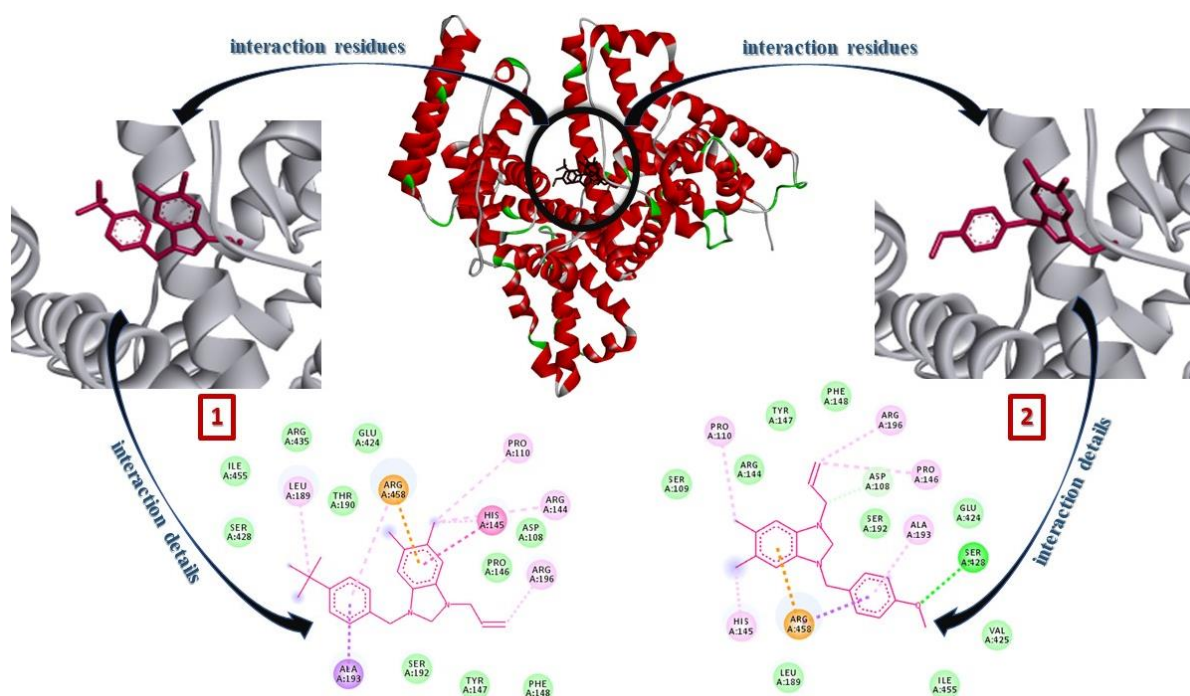


**Figure 8.** Interaction Residue (middle), Docking Conformations (grey), and Interaction Type of Benzimidazole Type 1, and 2 with Bovine Serum Albumin Crystal Structure

*Dark green and turquoise: H-bonds; green: van der Waals; Orange: pi-anion/cation; Pink: alkyl and pi-alkyl; Yellow: pi-sulfur; fuchsia: Pi-pi stacked and pi-pi T shaped*

The interaction of both molecules with bovine serum albumin was investigated by using molecular docking methods for examination of the interaction region and interaction size. Both molecules interact with approximately the same region of the serum albumin except small orientation

differences. 2 can interact as H-bonds through the methoxy group. The interaction regions and details of the molecules are presented in Figure 8.

**Table 2.** Active Sites of Bovine Serum Albumin (PDB ID:4f5s) with 1, and 2

Molecules	Bind. Aff.*	Amino Acids Residue
1	-8.07	Arg458, Ala193, His145, Pro110, Arg144, Leu189, Arg196, Tyr147, Phe148, Thr190, Ser192, Glu424, Ser428, Arg435, Ile455
2	-7.36	Asp108, Ser428, Arg458, Pro110, His145, Pro146, Arg196, Ser109, Arg144, Tyr147, Phe148, Leu189, Ser192, Glu424, Val425, Ile455

\*kcal/mol; red: H-bond, green: pi interactions, blue: Van der Waals interactions

Interaction regions, types, and magnitudes of molecules with macromolecules can be examined by molecular docking methods. 1 performs pi- and van der Waals-interactions with Bovine Serum Albumin. A binding affinity of -8.07 kcal/mol was determined by the pi-interactions with Arg458, Ala193, His145, Pro110, Arg144, Leu189, Arg196, and Van der Waals interactions. Due to the methoxy group substituted for the benzyl group of the 2, the H-bond, which is considered important in such analysis, was recorded with Asp108, and Ser428. The pi-interactions with Arg458, Pro110, His145, Pro146, and Arg196 are also noteworthy. The binding affinity calculated as a result of the contribution of many Van der Waals interactions to these interactions was determined as -7.36 kcal/mol (Table 2).

Examining the interactions of N-heterocyclic carbene molecules with BSA by molecular docking methods is not very common in the literature. However, analysis of transition metal complexes containing NHC-derived ligands is quite common. Rani et al. (2021) analyzed the Ni(II) complexes with NHC type ligands and the results of docking studies reveal that the binding energy ranging from -6.52 to -8.05 kcal mol<sup>-1</sup> towards the target BSA protein were recorded. Also, Feizi-Dehnavybi et al. (2021) recorded that BSA forms a hydrogen bond with His246 residue with the length of 3 Å and there are van der Waals forces between Pd(II) complex and Ser104, Lys106, Tyr147, Leu103, Ile202, Cys245, Gly247, Lys242 and Gln203 residues. Alinaghi et al. (2020) published that a hydrogen bond between the Pd(II) complex oxygen atom and Glu 125 (2.2 Å) is observed. In the same paper, the amino acid residues of BSA, which interacted with the complex, are Phe36, Pro113, Lys114, Leu115, Lys116, Leu122, Glu125, Phe133, Lys136, Tyr139 and Tyr160. It is common that the metal complexes of the NHC molecules could have better binding results than the individual NHC molecules. But the calculated result for the studied molecules in this research have better binding affinities than the complex molecules.

## Conclusions

Serum albumin is important since it is the most abundant protein in the blood and has many activities. Analysis of the interactions of pharmaceutical molecules with blood proteins is an important research area. The use of computational methods is useful in examining these kinds of interactions. It is recorded that 1 shows better pharmaceutical activity according to the results of both structural and molecular docking analyses. Since molecules are analyzed relatively in theoretical calculations, it is important to reproduce the structural and interactional analyzes of different substituted species, since the analysis of more molecules will help to decide on the molecules that will pass to the experimental stage.

## Author Contribution

Elvan Üstün performed the data collection and theoretical analysis. Neslihan Şahin performed the experimental process. The authors read and approved the article.

## Ethic

There are no ethical issues with the publication of this article.

### Conflict of interest

The authors declare that they have no known competing financial interests or personal relationships that could have appeared to influence the work reported in this paper.

### ORCID

Elvan Üstün  <https://orcid.org/0000-0002-0587-7261>

Neslihan Şahin  <https://orcid.org/0000-0003-1498-4170>

### References

- Alinaghi, M., Karami, K., Shahpiri, A., Momtazi-Borojeni, A. A., Abdollahi, E., & Lipkowski, J. (2020). A Pd (II) complex derived from pyridine-2-carbaldehyde oxime ligand: Synthesis, characterization, DNA and BSA interaction studies and in vitro anticancer activity. *Journal of Molecular Structure*, 1219, 128479. <https://doi.org/10.1016/j.molstruc.2020.128479>
- Arduengo III, A. J., Harlow, R. L., & Kline, M. (1991). A stable crystalline carbene. *Journal of the American Chemical Society*, 113(1), 361-363. <https://doi.org/10.1021/ja00001a054>
- Becke, A. D. (1988). Correlation energy of an inhomogeneous electron gas: A coordinate-space model. *The Journal of Chemical Physics*, 88(2), 1053-1062. <https://doi.org/10.1063/1.454274>
- Bejaoui, L., Brahmia, A., Marzouki, R., Dusek, M., Eigner, V., Serdaroğlu, G., ... & Hassen, R. B. (2020). Synthesis, crystal structure, hirshfeld surface analysis, spectroscopic, biological and first-principles studies of novel aminocoumarins. *Journal of Molecular Structure*, 1221, 128862. <https://doi.org/10.1016/j.molstruc.2020.128862>
- Bujacz, A. (2012). Structures of bovine, equine and leporine serum albumin. *Acta Crystallographica Section D: Biological Crystallography*, 68(10), 1278-1289. <https://doi.org/10.1107/S0907444912027047>
- Dassault Systèmes BIOVIA (2016). *Discovery studio modeling environment, release 2017*. Dassault Systèmes.
- Feizi-Dehnaneybi, M., Dehghanian, E., & Mansouri-Torshizi, H. (2021). A novel palladium (II) antitumor agent: Synthesis, characterization, DFT perspective, CT-DNA and BSA interaction studies via in-vitro and in-silico approaches. *Spectrochimica Acta Part A: Molecular and Biomolecular Spectroscopy*, 249, 119215. <https://doi.org/10.1016/j.saa.2020.119215>
- Furche, F., & Perdew, J. P. (2006). The performance of semilocal and hybrid density functionals in 3 d transition-metal chemistry. *The Journal of Chemical Physics*, 124(4), 044103. <https://doi.org/10.1063/1.2162161>
- Goldwasser, P., & Feldman, J. (1997). Association of serum albumin and mortality risk. *Journal of Clinical Epidemiology*, 50(6), 693-703. [https://doi.org/10.1016/S0895-4356\(97\)00015-2](https://doi.org/10.1016/S0895-4356(97)00015-2)
- Law, C. S., & Yeong, K. Y. (2021). Benzimidazoles in drug discovery: A patent review. *ChemMedChem*, 16(12), 1861-1877. <https://doi.org/10.1002/cmdc.202100004>
- Manoharan, S., & Anandan, S. (2014). Cyanovinyl substituted benzimidazole based (D-π-A) organic dyes for fabrication of dye sensitized solar cells. *Dyes and Pigments*, 105, 223-231. <https://doi.org/10.1016/j.dyepig.2014.02.010>
- Nair, V., Vellalath, S., & Babu, B. P. (2008). Recent advances in carbon-carbon bond-forming reactions involving homoenolates generated by NHC catalysis. *Chemical Society Reviews*, 37(12), 2691-2698. <https://doi.org/10.1039/B719083M>

- Narasimhan, B., Sharma, D., & Kumar, P. (2012). Benzimidazole: A medicinally important heterocyclic moiety. *Medicinal Chemistry Research*, 21(3), 269-283. <https://doi.org/10.1007/s00044-010-9533-9>
- Neese, F. (2012). The ORCA program system. *Wiley Interdisciplinary Reviews: Computational Molecular Science*, 2(1), 73-78. <https://doi.org/10.1002/wcms.81>
- Neese, F. (2018). Software update: the ORCA program system, version 4.0. *Wiley Interdisciplinary Reviews: Computational Molecular Science*, 8(1), e1327. <https://doi.org/10.1002/wcms.1327>
- P Barot, K., Nikolova, S., Ivanov, I., & D Ghate, M. (2013). Novel research strategies of benzimidazole derivatives: a review. *Mini reviews in Medicinal Chemistry*, 13(10), 1421-1447. <https://www.ingentaconnect.com/content/ben/mrmc/2013/00000013/00000010/art00005>
- Perepichka, D. F., & Bryce, M. R. (2005). Molecules with exceptionally small HOMO–LUMO gaps. *Angewandte Chemie International Edition*, 44(34), 5370-5373. <https://doi.org/10.1002/anie.200500413>
- Peters Jr, T. (1985). Serum albumin. *Advances in Protein Chemistry*, 37, 161-245. [https://doi.org/10.1016/S0065-3233\(08\)60065-0](https://doi.org/10.1016/S0065-3233(08)60065-0)
- Phillips, J. C. (1961). Generalized Koopmans' Theorem. *Physical Review*, 123(2), 420. <https://doi.org/10.1103/PhysRev.123.420>
- Rani, J. J., Jayaseeli, A. M. I., Rajagopal, S., Seenithurai, S., Chai, J. D., Raja, J. D., & Rajasekaran, R. (2021). Synthesis, characterization, antimicrobial, BSA binding, DFT calculation, molecular docking and cytotoxicity of Ni (II) complexes with Schiff base ligands. *Journal of Molecular Liquids*, 328, 115457. <https://doi.org/10.1016/j.molliq.2021.115457>
- Şahin, N., Üstün, E., Tutar, U., Çelik, C., Gürbüz, N., & Özdemir, İ. (2021). Antimicrobial activity, inhibition of biofilm formation, and molecular docking study of novel Ag-NHC complexes. *Journal of Organometallic Chemistry*, 954, 122082. <https://doi.org/10.1016/j.jorganchem.2021.122082>
- Serdaroğlu, G., Şahin, N., Şahin-Bölükbaşı, S., & Üstün, E. (2022). Novel Ag (I)-NHC complex: Synthesis, in vitro cytotoxic activity, molecular docking, and quantum chemical studies. *Zeitschrift für Naturforschung C*, 77(1-2), 21-36. <https://doi.org/10.1515/znc-2021-0130>
- Serdaroğlu, G., Şahin, N., Üstün, E., Tahir, M. N., Arıcı, C., Gürbüz, N., & Özdemir, İ. (2021). PEPPSI type complexes: Synthesis, x-ray structures, spectral studies, molecular docking and theoretical investigations. *Polyhedron*, 204, 115281. <https://doi.org/10.1016/j.poly.2021.115281>
- Spasov, A. A., Yozhitsa, I. N., Bugaeva, L. I., & Anisimova, V. A. (1999). Benzimidazole derivatives: Spectrum of pharmacological activity and toxicological properties (A review). *Pharmaceutical Chemistry Journal*, 33(5), 232-243. <https://doi.org/10.1007/BF02510042>
- Velık, J., Baliharova, V., Fink-Gremmels, J., Bull, S., Lamka, J., & Skálová, L. (2004). Benzimidazole drugs and modulation of biotransformation enzymes. *Research in Veterinary Science*, 76(2), 95-108. <https://doi.org/10.1016/j.rvsc.2003.08.005>
- Vijayaraj, R., Subramanian, V., & Chattaraj, P. K. (2009). Comparison of global reactivity descriptors calculated using various density functionals: A QSAR perspective. *Journal of Chemical Theory and Computation*, 5(10), 2744-2753. <https://doi.org/10.1021/ct900347f>
- Yadav, G., & Ganguly, S. (2015). Structure activity relationship (SAR) study of benzimidazole scaffold for different biological activities: A mini-review. *European Journal of Medicinal Chemistry*, 97, 419-443. <https://doi.org/10.1016/j.ejmech.2014.11.053>